

# lncRNA MIRF Promotes Cardiac Apoptosis through the miR-26a-Bak1 Axis

Xiaomin Su,<sup>1,2,5</sup> Lifang Lv,<sup>1,3,5</sup> Yue Li,<sup>1,2</sup> Ruonan Fang,<sup>1,2</sup> Rui Yang,<sup>1</sup> Chao Li,<sup>1</sup> Tianyu Li,<sup>1,2</sup> Di Zhu,<sup>1</sup> Xuelian Li,<sup>1</sup> Yuhong Zhou,<sup>1</sup> Hongli Shan,<sup>1,2,4</sup> and Haihai Liang<sup>1,2,4</sup>

<sup>1</sup>Department of Pharmacology (State-Province Key Laboratories of Biomedicine-Pharmaceutics of China, Key Laboratory of Cardiovascular Research, Ministry of Education), College of Pharmacy, Harbin Medical University, Harbin, Heilongjiang 150081, P. R. China; <sup>2</sup>Northern Translational Medicine Research and Cooperation Center, Heilongjiang Academy of Medical Sciences, Harbin Medical University, Harbin, Heilongjiang 150081, P. R. China; <sup>3</sup>The Centre of Functional Experiment Teaching, Department of Basic Medicine, Harbin Medical University, Harbin, Heilongjiang 150081, P. R. China; <sup>4</sup>Research Unit of Noninfectious Chronic Diseases in Frigid Zone (2019RU070), Chinese Academy of Medical Sciences, Heilongjiang 150081, P. R. China

**Acute myocardial infarction (AMI) is the leading cause of death worldwide. Identifying the pathways that block cardiac cell death is a therapeutic strategy for ischemic heart disease. We found that long noncoding RNA (lncRNA) myocardial infarction-regulatory factor (MIRF) promoted ischemic myocardial injury by regulating autophagy through targeting miR-26a. However, the role of MIRF-miR-26a in apoptosis during AMI has not been delineated. In this study, we found the down-regulation of miR-26a both in the heart of myocardial infarction (MI) mice and in H<sub>2</sub>O<sub>2</sub>-treated cardiomyocytes. miR-26a silencing resulted in apoptosis, whereas overexpression of miR-26a attenuated H<sub>2</sub>O<sub>2</sub>-induced apoptosis through promoting mitochondrial ATP content and increasing mitochondrial membrane potential (MMP). Moreover, forced expression of miR-26a protected against MI-induced cardiac injury and attenuated cardiac apoptosis. Further studies showed that miR-26a inhibited apoptosis through regulation of Bak1. Furthermore, MIRF decreased ATP content and MMP through regulating miR-26a, which then promoted the cardiomyocyte apoptosis. In contrast, deficiency of MIRF promoted mitochondrial ATP content and increased MMP, and then inhibited MI or H<sub>2</sub>O<sub>2</sub>-induced cardiac apoptosis, which was abolished by miR-26a inhibitor. Taken together, these results suggested that MIRF contributed to cardiomyocyte apoptosis through modulating Bak1 by regulation of miR-26a, which can be a potential therapeutic target for the treatment of ischemic heart disease.**

## INTRODUCTION

Acute myocardial infarction (AMI) is one of the major causes of morbidity and mortality worldwide.<sup>1</sup> During AMI, cardiomyocytes suffer from hypoxia, which induces a severe inflammatory response,<sup>2</sup> subsequently promotes myocytes apoptosis and cardiac fibrosis, and finally leads to a worse cardiac function, even heart failure.<sup>3,4</sup> Cardiomyocyte apoptosis is the most common phenomenon among all kinds of cardiac diseases, which is mediated by intrinsic, extrinsic, and endoplasmic reticulum pathways through pro-apoptotic or anti-apoptotic molecules.<sup>5,6</sup> Thus, it is valuable to prevent cardiomyocyte apoptosis for cardiac disease, especially for ischemic cardiac

disease. However, the molecular components involved in regulating programmed apoptosis in the heart remain largely unidentified.

Noncoding RNAs (ncRNAs), a class of RNAs that do not encode proteins but function as key molecules for cell processes,<sup>7</sup> are divided into long noncoding RNAs (lncRNAs), microRNAs (miRNAs), tRNAs, rRNAs, Piwi-interacting RNA (piRNAs), guide RNA (gRNAs), small nuclear RNAs (snRNAs), circular RNAs (circRNAs), small interfering RNAs (siRNAs), and small nucleolar RNAs (snoRNAs) according to their length, function, and structure.<sup>8</sup> Recent studies mainly focused on lncRNAs, miRNAs, and circRNAs, which have been proved to play a crucial role in multiple cell processes, including cell cycle, cell proliferation, cell invasion, and cell death.<sup>9,10</sup> Accumulating evidence shows that lncRNAs and miRNAs regulate fundamental molecules associated with cardiomyocyte apoptosis, as well as ischemic cardiac diseases. lncRNA CARL inhibited anoxia-induced mitochondrial fission and apoptosis in cardiomyocytes through regulating miR-539 and decreased the expression of PHB2.<sup>11</sup> The lncRNA Mhrt-Nrf2-dependent pathway attenuated doxorubicin-induced cardiomyocyte apoptosis and cardiac dysfunction.<sup>12</sup> In addition, reduction of the expression of lncRNA UCA1 promoted cardiomyocyte apoptosis partially through stimulation of p27 expression.<sup>13</sup>

Bak1 is a member of the proapoptotic Bcl-2 family, which can be antagonized by antiapoptotic members such as Bcl-2.<sup>14</sup> In response to an apoptotic stimulus, activated BH3-only proteins directly induce a conformational change of Bak1, which subsequently oligomerize and insert into the mitochondrial membrane, where they form pores either by themselves or by associating with the permeability transition pore complex.<sup>14</sup> Consequently, proapoptotic factors are released from

Received 14 February 2020; accepted 1 May 2020;  
<https://doi.org/10.1016/j.omtn.2020.05.002>.

<sup>5</sup>These authors contributed equally to this work.

**Correspondence:** Haihai Liang, Department of Pharmacology (State-Province Key Laboratories of Biomedicine-Pharmaceutics of China, Key Laboratory of Cardiovascular Research, Ministry of Education), College of Pharmacy, Harbin Medical University, Baojian Road 157, Harbin, Heilongjiang 150081, P. R. China.  
E-mail: [lianghaihai@ems.hrbmu.edu.cn](mailto:lianghaihai@ems.hrbmu.edu.cn)



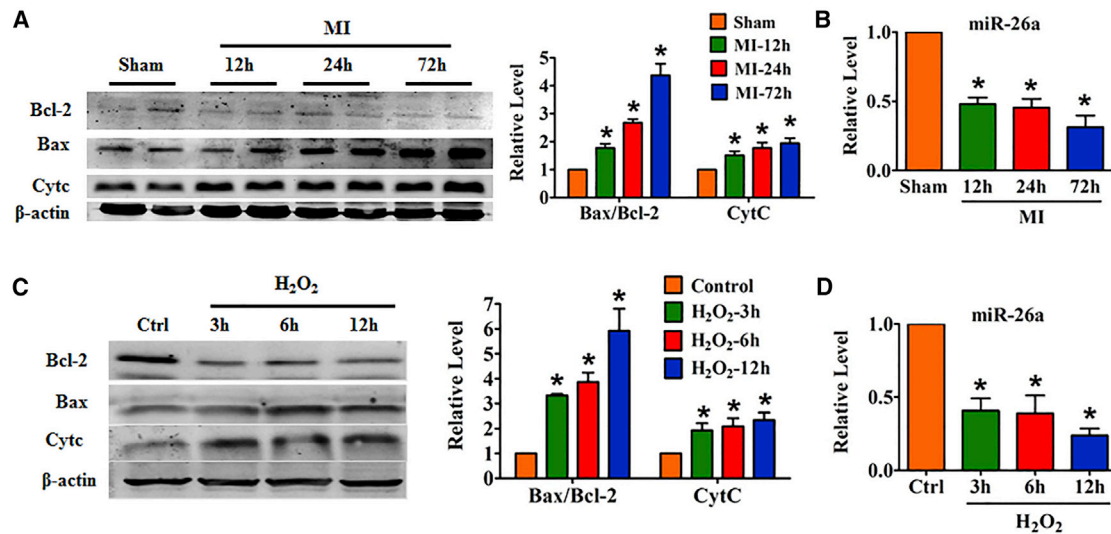


**Figure 1. Downregulation of miR-26a during Cardiac Injury *In Vivo* and *In Vitro***

(A) Dysregulation of apoptosis-relevant proteins in a mouse model of myocardial infarction (MI).  $n = 4$ ; \* $p < 0.05$  versus sham. (B) Downregulation of miR-26a in the heart of MI mice.  $n = 6$ ; \* $p < 0.05$  versus sham. (C) Dysregulation of apoptosis-relevant proteins in a cellular model of oxidative stress by H<sub>2</sub>O<sub>2</sub> in cultured neonatal mouse cardiomyocytes (NMCMs).  $n = 3$ ; \* $p < 0.05$  versus control. (D) Downregulation of miR-26a in H<sub>2</sub>O<sub>2</sub>-treated NMCMs.  $n = 4$ ; \* $p < 0.05$  versus control.

the inner mitochondrial membrane into the cytosol, such as cytochrome *c* (CytC), which contributes to the formation of the apoptosome and subsequent activation of the caspase cascade.<sup>15,16</sup> It has been reported that Bak1 was a target of miR-125b-5p, and miR-125b-5p protected the heart from myocardial infarction (MI) by repressing pro-apoptotic Bak1 in cardiomyocytes.<sup>17</sup>

In a previous study, we found that lncRNA MIRF participated in AMI by regulating Usp15 through acting as a competing endogenous RNA (ceRNA) for miR-26a.<sup>18</sup> Both apoptosis and autophagy are essential processes during AMI; thus, we want to further explore whether the MIRF-miR26a axis regulates cardiomyocyte apoptosis during AMI. In this study, our results showed that lncRNA MIRF contributed to cardiomyocyte apoptosis by modulating miR-26a, and then promoted the expression of pro-apoptotic protein Bak1. Our finding provides new insight into the roles of lncRNAs and miRNAs in the development of AMI.

## RESULTS

### Silencing miR-26a Promotes Cardiac Apoptosis *In Vitro* and *In Vivo*

To determine the function of miR-26a in MI, we generated an MI mouse model. As shown in Figure 1A, the expression of anti-apoptotic protein Bcl-2 was decreased, whereas the expressions of pro-apoptotic proteins Bax and CytC were increased in MI mice, which suggested an increase of apoptosis level. Meanwhile, we found that the expression of miR-26a was decreased in the hearts of MI mice (Figure 1B). To further examine the role of miR-26a during cardiomyocytes injury, we used 200  $\mu$ M H<sub>2</sub>O<sub>2</sub> to induce neonatal mouse cardiomyocytes (NMCMs) injury. In keeping with *in vivo* results, H<sub>2</sub>O<sub>2</sub> treatment inhibited the expression of Bcl-2, but increased the expression of Bax and CytC at

protein levels (Figure 1C). Thus, H<sub>2</sub>O<sub>2</sub> treatment induced a time-dependent cardiomyocyte apoptosis. Furthermore, miR-26a level was also decreased in H<sub>2</sub>O<sub>2</sub>-treated cardiomyocytes with time dependence (Figure 1D). These results showed that miR-26a was decreased during cardiac injury, along with a high level of cardiac apoptosis.

To further identify the function of miR-26a in the MI process, we generated miR-26a sponge transgenic mice (KD-miR-26a mice) to knock down the expression of endogenous miR-26a. As illustrated in Figure 2A, knockdown (KD) of miR-26a decreased Bcl-2 protein level but increased Bax and CytC protein levels, indicating that KD of miR-26a promoted cardiac apoptosis. Also, TUNEL staining showed a significant increase of TUNEL-positive cell numbers in KD-miR-26a mice (Figure 2B). Then, we knocked down miR-26a expression in NMCMs by using AMO-26a (Figure 2C); the western blot analysis showed that deficiency of miR-26a decreased Bcl-2 expression but increased Bax and CytC expression levels (Figure 2D). At the same time, loss of miR-26a increased caspase-3 activity (Figure 2E). Furthermore, silencing of miR-26a increased the numbers of TUNEL-positive cells (Figure 2F). Taken together, inhibition of miR-26a induced cardiomyocyte apoptosis.

### Overexpression of miR-26a Protects against Cardiac Injury by Inhibiting Cardiac Apoptosis

To examine whether enhancing miR-26a expression could protect against cardiac apoptosis, we transfected NMCMs with miR-26a mimics to enhance miR-26a expression *in vitro* (Figure 3A) and exposed them to 200  $\mu$ M H<sub>2</sub>O<sub>2</sub> for 12 h. miR-26a removed the detrimental effect of H<sub>2</sub>O<sub>2</sub> on cardiomyocyte apoptosis with an increase of Bcl-2 level and a decrease of Bax and CytC expression (Figure 3B). Additionally, TUNEL analysis showed that overexpression of miR-26a, but

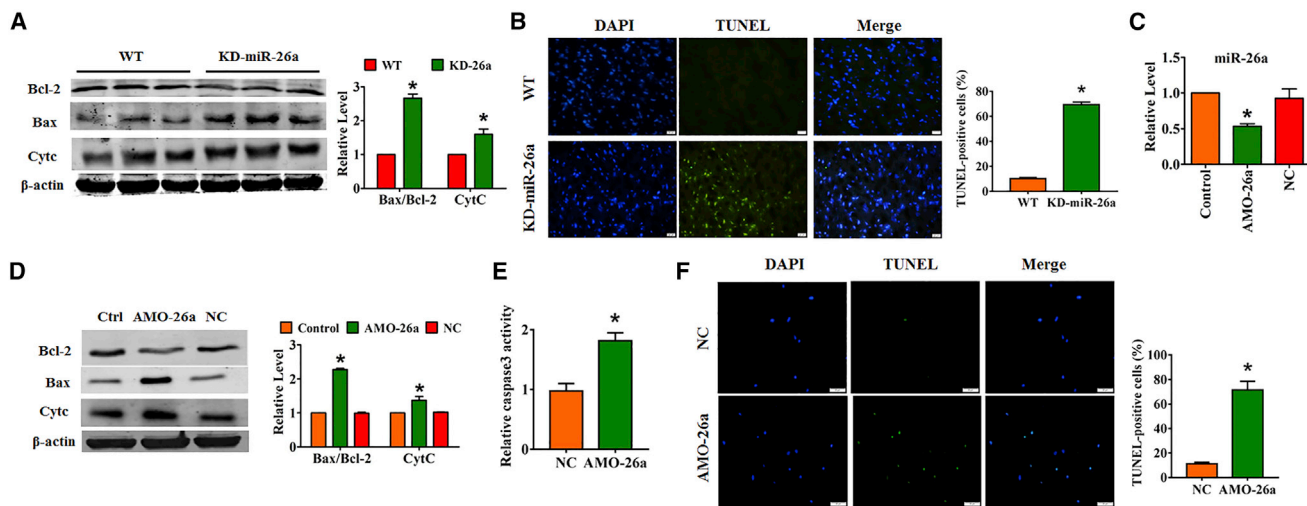


**Figure 2. Knockdown of miR-26a Results in Apoptosis *In Vivo* and *In Vitro***

(A) Knockdown of miR-26a led to the upregulation of Bax and CytC, and downregulation of Bcl-2 in mice.  $n = 3$ ;  $*p < 0.05$  versus WT. (B) TUNEL staining was used to detect the cardiac apoptosis of mouse heart. Green, TUNEL-positive cardiomyocytes; blue, DAPI. Scale bars: 20  $\mu\text{m}$ .  $*p < 0.05$ ;  $n = 3$ . (C) Quantitative real-time PCR determines the expression of miR-26a in NCMs after transfection of AMO-26a.  $n = 4$ ;  $*p < 0.05$  versus control. (D) Silencing miR-26a increased the expression of Bax and CytC, but decreased the expression of Bcl-2 at protein levels in NCMs.  $n = 3$ ;  $*p < 0.05$  versus control. (E) The activity of caspase-3 in cardiomyocytes.  $*p < 0.05$ ;  $n = 4$ . (F) Proapoptotic effects of miR-26a inhibition in NCMs, as revealed by TUNEL staining of chromosome fragmentation.

not negative control (NC), reversed  $\text{H}_2\text{O}_2$ -induced cardiomyocyte apoptosis (Figure 3C). Mitochondria are the place not only for producing ATP, but also for apoptosis in cardiomyocytes, and we detected the mitochondrial ATP content to reflect the state of mitochondria in NCMs.  $\text{H}_2\text{O}_2$  treatment significantly decreased the ATP content, and this effect was reversed by miR-26a mimics, but not NC (Figure 3D). We then evaluated the effect of miR-26a on mitochondrial membrane potential (MMP) by JC-1 staining. As illustrated in Figure 3E,  $\text{H}_2\text{O}_2$  induced depolarization of the MMP, as indicated by an enhancement of JC-1 staining, and this effect was attenuated by miR-26a.

Next, we injected agomiR-26a into mice through the tail vein to enhance miR-26a expression (Figure 3F). At the third day after injection, the mice were subjected to MI surgery for 24 h. We used transmission electron microscopy (TEM) to detect ultrastructural damage of cardiomyocytes. As shown in Figure 3G, the mitochondria swelling, broken myofibril, and nucleus dissolution occurred in cardiomyocytes of MI mice, but these damages were greatly ameliorated after agomiR-26a injection. The western blot analysis showed that agomiR-26a injection inhibited MI-induced cardiac apoptosis by increasing Bcl-2 level and decreasing Bax and CytC expression (Figure 3H). We evaluated cardiac apoptosis using TUNEL staining and found that overexpression of miR-26a reduced the number of apoptotic myocytes (Figure 3I). These data suggested that miR-26a protected against cardiac injury by inhibiting apoptosis in cardiomyocytes.

#### Bak1 Is One of the Direct Targets of miR-26a during Cardiomyocyte Apoptosis

To elucidate the mechanisms underlying the above phenomenon, we attempted to identify the target genes of miR-26a. The results of

TargetScan predicted that the 3' UTR of Bak1 possessed a directed target site for miR-26a (Figure 4A). Bak1 is a proapoptotic gene and is involved in cardiac apoptosis and MI. The expression of Bak1 rose both in MI-induced cardiac injury and in  $\text{H}_2\text{O}_2$ -induced cardiomyocytes damage with a time-dependent manner (Figures 4B and 4C). To investigate whether miR-26a targeted on Bak1, we performed dual-luciferase reporter assay in the HEK293 cell line and found that the luciferase activity of the wild-type (WT) 3' UTR of Bak1 was significantly repressed in the miR-26a mimic group compared with the NC group, and this effect was removed by AMO-26a (Figure 4D). However, miR-26a had no effect on the luciferase activity of mutant 3' UTR of Bak1 (Figure 4D). Moreover, quantitative real-time PCR analysis showed that miR-26a or AMO-26a had no effect on the mRNA expression of Bak1 (Figure 4E). In addition, overexpression of miR-26a inhibited, whereas silencing miR-26a increased, the expression of Bak1 at the protein level in NCMs (Figures 4F and 4G). Furthermore, the protein level of Bak1 was upregulated in the hearts of miR-26a KD mice (Figure 4H).

#### Role of lncRNA MIRF as a ceRNA for miR-26a to Promote Cardiac Apoptosis

Our previous study had found that the expression and activity of miR-26a was regulated by lncRNA MIRF during MI.<sup>18</sup> We thus further investigate the effect of MIRF on cardiomyocyte apoptosis. As shown in Figure 5A, overexpression of MIRF increased TUNEL-positive cell numbers compared with pcDNA3.1, while this effect was partly alleviated by miR-26a. Meanwhile, overexpression of MIRF decreased antiapoptotic protein Bcl-2 expression and increased proapoptotic protein Bax, CytC, and Bak1 expression and caspase-3 activity in NCMs, which was restored after forced expression of miR-26a (Figures 5B and 5C).

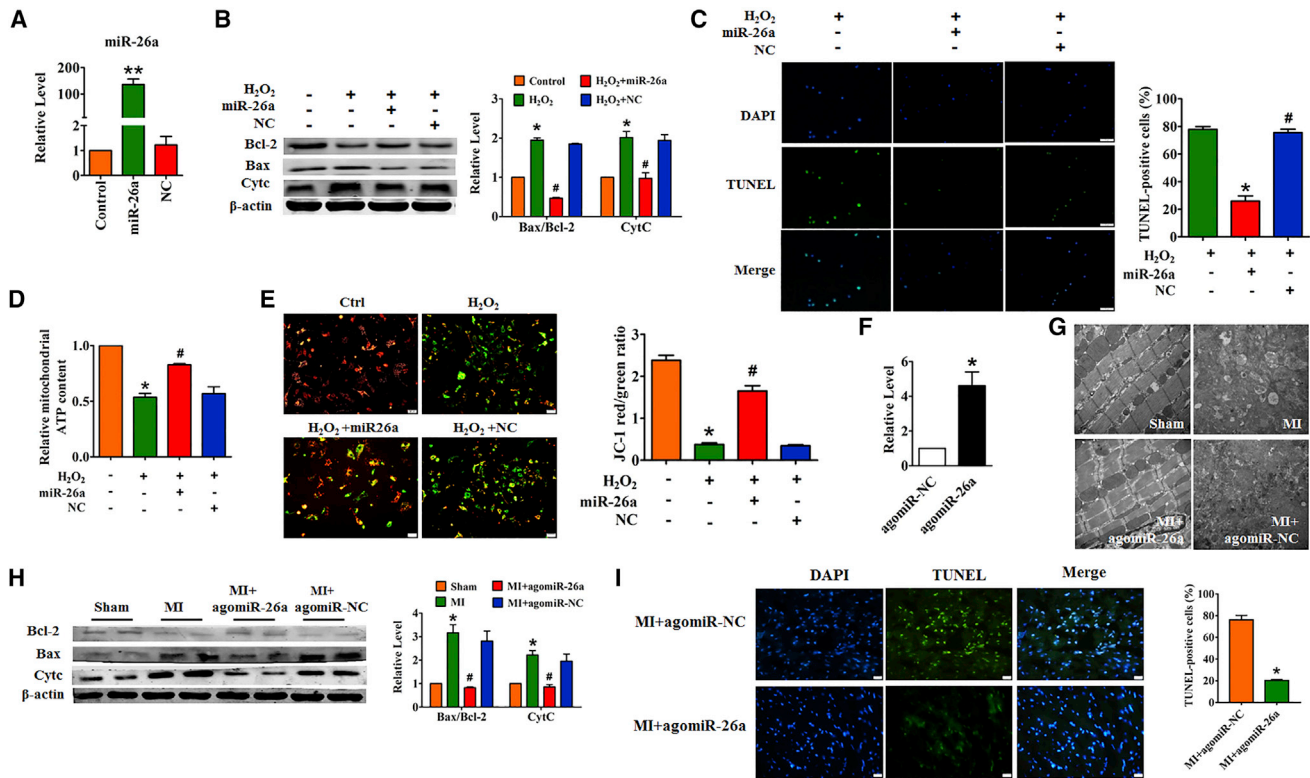


**Figure 3. Overexpression of miR-26a Alleviates Apoptosis in MI Mice and in H<sub>2</sub>O<sub>2</sub>-Treated NCMCs**

(A) Quantitative real-time PCR analysis of miR-26a expression in NCMCs transfected with miR-26a.  $n = 3$ ; \*\* $p < 0.01$  versus control. (B) Bcl-2, Bax, and CytC protein levels were detected by immunoblotting.  $n = 3$ ; \* $p < 0.05$  versus control, # $p < 0.05$  versus H<sub>2</sub>O<sub>2</sub>. (C) TUNEL staining was applied to examine the effects of miR-26a on H<sub>2</sub>O<sub>2</sub>-induced NCMC apoptosis. Green, TUNEL-positive cardiomyocytes; blue, DAPI. Scale bars: 20  $\mu$ m. (D) Cardiomyocytes ATP content was determined using ATP assay and normalized to protein amount.  $n = 4$ ; \* $p < 0.05$  versus Ctrl, # $p < 0.05$  versus H<sub>2</sub>O<sub>2</sub>. (E) MMP was identified by JC-1 staining. Red fluorescence represented normal MMP, whereas green fluorescence was indicative of damaged mitochondrial potential. (F) Quantitative real-time PCR assay showed the upregulation of miR-26a in the heart of mice after injection of agomiR-26a.  $n = 5$ ; \* $p < 0.05$  versus agomiR-NC. (G) TEM was performed to detect the ultrastructure of cardiomyocytes of heart tissues from mice treated with agomiR-NC or agomiR-26a after MI surgery. (H) Immunoblot analysis showed the protein expression of Bcl-2, Bax, and CytC.  $n = 4$ ; \* $p < 0.05$  versus sham, # $p < 0.05$  versus MI. NCMCs were cultured and transfected with miR-26a mimics and NC, then exposed to 200  $\mu$ M H<sub>2</sub>O<sub>2</sub> for 12 h. (I) Representative images of TUNEL staining showing apoptotic cells (stained in green) in cardiomyocytes. The nuclei were stained blue with DAPI. \* $p < 0.05$ ;  $n = 3$ .

Moreover, MIRF inhibited the mitochondria function that was exhibited by mitochondria ATP content assay (Figure 5D). Furthermore, forced expression of miR-26a mitigated the inhibition of mitochondrial function by MIRF (Figures 5D and 5E). These results indicated that MIRF induced cardiomyocyte apoptosis by inhibiting the function of miR-26a.

#### Loss of MIRF Attenuates Cardiomyocyte Apoptosis through Modulating miR-26a

We then applied MIRF siRNA to examine whether silencing MIRF could alleviate H<sub>2</sub>O<sub>2</sub>-induced cardiomyocyte apoptosis. As shown in Figure 6A, 200  $\mu$ M H<sub>2</sub>O<sub>2</sub> treatment induced a significant apoptosis in NCMCs, an effect that was alleviated by silencing MIRF, whereas inhibition of miR-26a abolished the beneficial action of MIRF KD. Western blot analysis showed that KD of MIRF restored H<sub>2</sub>O<sub>2</sub>-induced upregulation of Bax, Bak1, and CytC and downregulation of Bcl-2 expression, and these changes were abated by silencing miR-26a (Figure 6B). Furthermore, silencing of MIRF mitigated the H<sub>2</sub>O<sub>2</sub>-induced inhibition of ATP and MMP in NCMCs, inhibition that was effectively

attenuated by addition of the miR-26a inhibitor (Figures 6C and 6D). These results suggested that deficiency of MIRF protected against H<sub>2</sub>O<sub>2</sub>-induced apoptosis by targeting miR-26a.

AAV9-sh-MIRF and AAV9-sh-Scramble were intravenously injected into mice subjected to MI for 24 h after injection to determine the potential cardioprotective effect of MIRF. TEM analysis showed an obvious improvement of myocyte structure after KD of MIRF, including mild mitochondrial swelling and broken myofilament compared with the MI group (Figure 7A). In addition, injection of AAV9-sh-MIRF, but not AAV9-sh-Scramble, abrogated MI-induced cardiac apoptosis, exhibiting an increase of Bcl-2 and a reduction of Bax, CytC, and Bak1 (Figure 7B). Compared with AAV9-sh-Scramble, AAV9-sh-MIRF decreased TUNEL-positive cells in MI hearts (Figure 7C).

#### DISCUSSION

In the present study, we found that lncRNA MIRF promoted cardiac apoptosis by regulating proapoptotic gene Bak1 through targeting

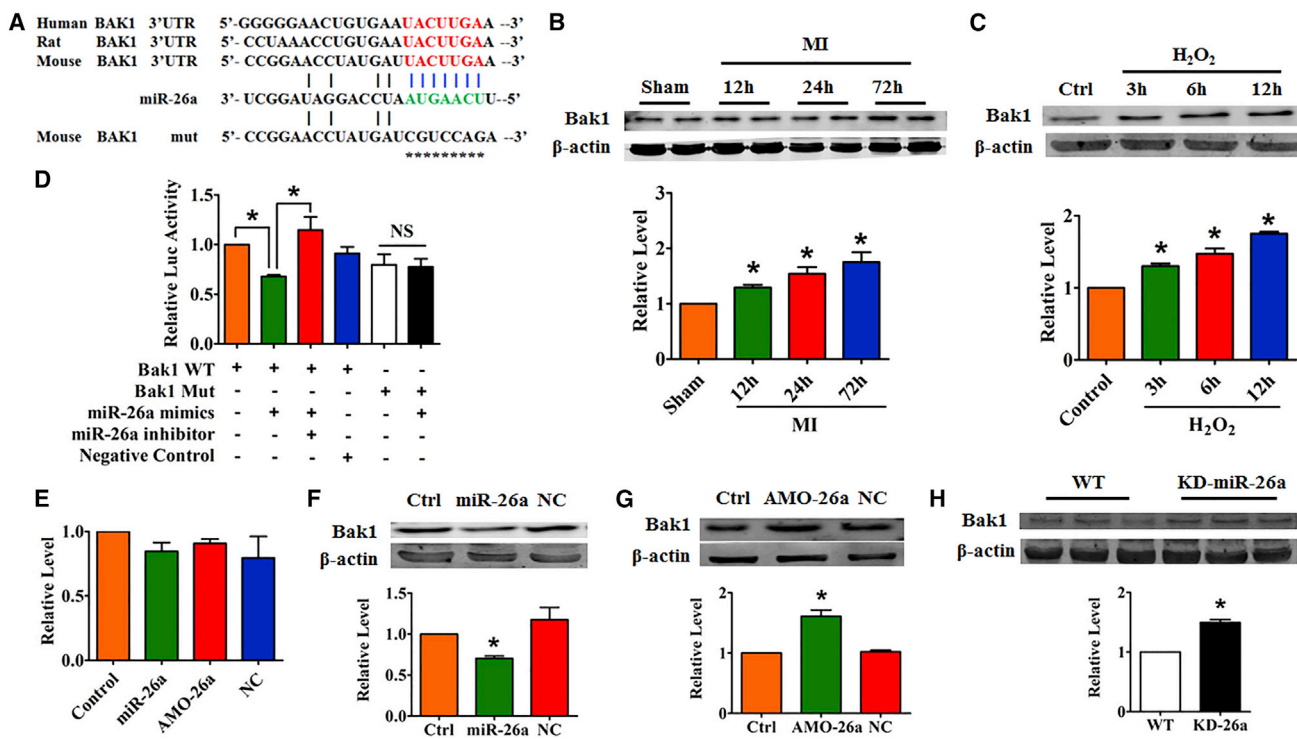


**Figure 4. Bak1 Is One of the Direct Targets of miR-26a**

(A) The sequence and binding sites of Bak1 and miR-26a in human, rat, and mouse. Bak1 was mutated into Bak1 mut with mutant binding bases with miR-26a. (B) The protein expression of Bak1 in the heart of MI mice. n = 4; \*p < 0.05 versus sham. (C) The protein expression of Bak1 in NMCMs treatment with H<sub>2</sub>O<sub>2</sub>. n = 3; \*p < 0.05 versus control. (D) HEK293 cells were transfected with WT or mutant Bak1 with or without miR-26a for 48 h. The luciferase activity was measured by dual-luciferase reporter assay system. n = 6; \*p < 0.05. (E) Quantitative real-time PCR was employed to determine the effect of miR-26a on Bak1 mRNA levels in NMCMs. n = 5. (F and G) The protein level of Bak1 was identified by western blot analysis in cultured cardiomyocytes. n = 3; \*p < 0.05 versus control. (H) The protein level of Bak1 was detected by western blot in the heart of WT and KD-miR-26a mice. n = 6; \*p < 0.05 versus WT.

miR-26a (Figure 7D). These findings revealed the molecular mechanism of the lncRNA MIRF-miR-26a-Bak1 axis on MI and suggested the potential clinical application of lncRNA MIRF and miR-26a for cardiovascular diseases.

Cardiovascular disease, especially MI, is one of the leading causes of hospitalization and death worldwide.<sup>19,20</sup> Thus, identifying molecular mechanisms and discovering impactful therapeutic targets are important for the treatment of cardiac injury. The fate of cardiac cells after ischemic injury is determined by the balance between cell survival and death.<sup>21</sup> Apoptosis is regarded as one cell death mechanism and can be induced by various stress conditions, such as oxidative stress and endoplasmic reticulum stress.<sup>22,23</sup> Following myocardial ischemic injury, cardiac apoptosis was dramatically enhanced, which has been widely demonstrated.<sup>24,25</sup> In our study, we found that Bax and CytC expression levels were increased, whereas Bcl-2 expression was decreased in the heart of MI mice or in H<sub>2</sub>O<sub>2</sub>-treated cardiomyocytes. Thus, it is valuable to prevent cardiomyocyte apoptosis during MI.

Accumulating evidence has shown the critical role of miRNAs in the pathogenesis of cardiovascular diseases.<sup>26,27</sup> It has been re-

ported that miR-21 could inhibit the expression of PDCD4 and attenuate cardiomyocyte apoptosis caused by ischemia/reperfusion injury.<sup>28</sup> In our previous study, we found that miR-26a was down-regulated during MI, and miR-26a participated in MI through regulating autophagy. Here, we also found that KD of miR-26a increased cardiac apoptosis level, exhibiting an increase of Bax and CytC and a decrease of Bcl-2 both *in vivo* and *in vitro*. Moreover, injection of agomiR-26a improved MI-impaired ultrastructure of cardiomyocytes and relieved MI-induced cardiac apoptosis. Because mitochondria are the major ATP and reactive oxygen species production organelles in cardiomyocytes, mitochondrial malfunction is tightly related to cardiac apoptosis and contributes to MI. We found that miR-26a could restore the mitochondrial ATP content and increase MMPs that were damaged during H<sub>2</sub>O<sub>2</sub> exposure.

Further studies explored the underlying mechanisms of miR-26a regulating cardiac apoptosis. It has been reported that miR-125b-5p protected the heart from AMI by repressing Bak1 expression in cardiomyocytes.<sup>17</sup> In our study, bioinformatic analysis showed that there were complementary bases between miR-26a and Bak1, and luciferase analysis showed that Bak1 was a direct target of miR-26a.

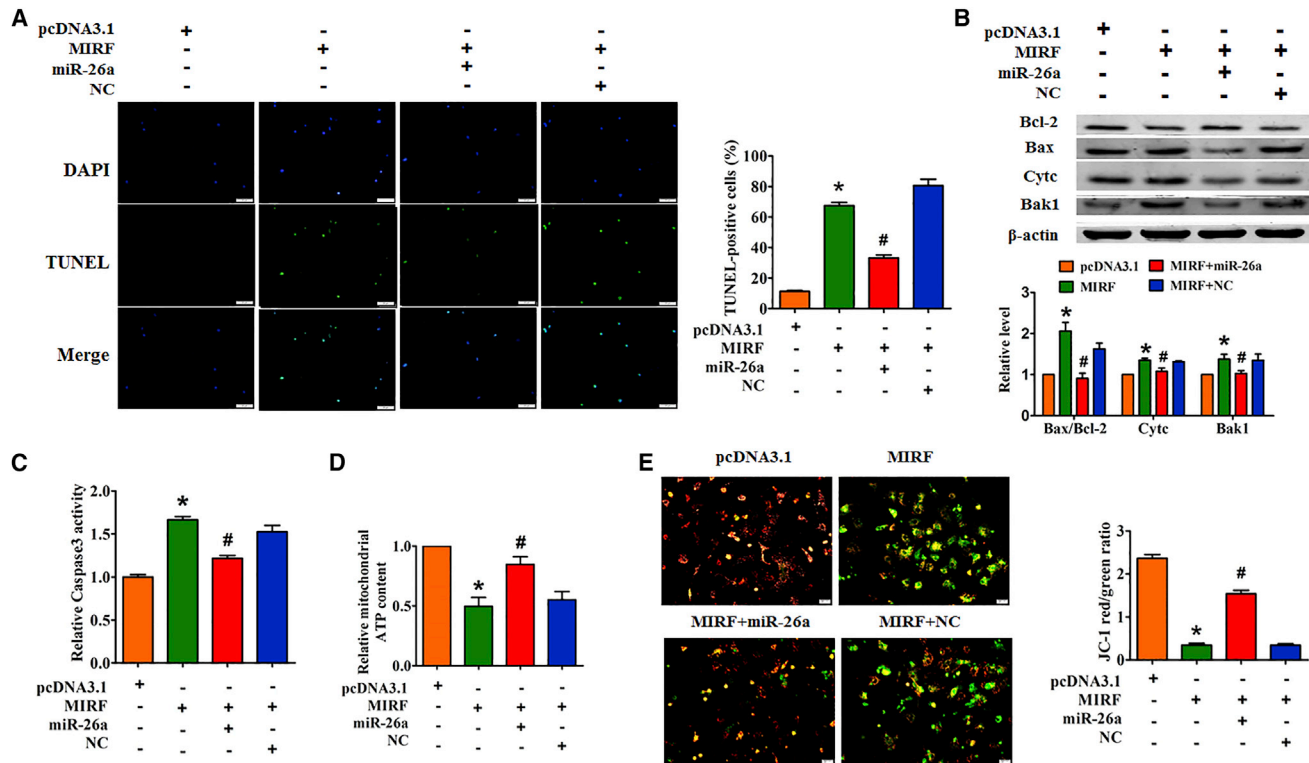


**Figure 5. Forced Expression of MIRF Promotes NCMs Apoptosis through Regulating miR-26a**

(A) TUNEL staining labeled apoptotic myocytes, and DAPI staining signed the nucleus. Scale bars: 20  $\mu\text{m}$ . \* $p < 0.05$  versus pcDNA3.1, # $p < 0.05$  versus MIRF. (B) Western blot analysis detected the expression of Bcl-2, Bax, and Cytc in cardiomyocytes.  $n = 3$ ; \* $p < 0.05$  versus pcDNA3.1, # $p < 0.05$  versus MIRF. (C) The activity of caspase-3 in cardiomyocytes.  $n = 4$ ; \* $p < 0.05$  versus pcDNA3.1, # $p < 0.05$  versus MIRF. (D) ATP content analysis detected the ATP content in mitochondria of cardiomyocyte, which indicated the function of mitochondria in cardiomyocyte.  $n = 4$ ; \* $p < 0.05$  versus pcDNA3.1, # $p < 0.05$  versus MIRF. (E) JC-1 staining indicated the MMP in cardiomyocytes. MIRF damaged mitochondrial potential, whereas miR-26a recovered MMP. \* $p < 0.05$  versus pcDNA3.1, # $p < 0.05$  versus MIRF.

Furthermore, miR-26a regulated Bak1 expression at the posttranscriptional level.

Increasing evidence suggested that lncRNA might function as pro-apoptotic or anti-apoptotic mediators.<sup>29</sup> It has been reported that KD of lncRNA-ZFAS1 protected cardiomyocytes against AMI via anti-apoptosis by regulating miR-150/CRP,<sup>30</sup> whereas lncRNA H19 protected H9C2 cells against hypoxia-induced apoptosis targeting miR-139.<sup>31</sup> Previously, we clarified that lncRNA MIRF acted as a ceRNA of miR-26a and modulated MI. Here, we found that lncRNA MIRF promoted cardiac apoptosis. Overexpression of lncRNA MIRF significantly increased TUNEL-positive cell numbers and elevated the expression of apoptosis-related proteins in cardiomyocytes. Moreover, lncRNA MIRF reduced mitochondrial ATP content and MMP in cardiomyocytes, which indicated the damage of mitochondrial function, and the disadvantaged effect of MIRF on apoptosis was abolished by miR-26a. On the contrary, loss of lncRNA MIRF alleviated MI- or  $\text{H}_2\text{O}_2$ -induced cardiomyocyte apoptosis and promoted the structure and function of mitochondria both *in vivo* and *in vitro*.

In conclusion, lncRNA MIRF inhibited the expression of miR-26a, which targeted on Bak1, leading to mitochondrial dysfunction and

cardiomyocyte apoptosis. Taken together, our results suggest that strategies of knocking down lncRNA MIRF or enhancing miR-26a should be further studied in cardiovascular diseases.

## MATERIALS AND METHODS

### Animal Treatment

C57BL/6 male mice (6–8 weeks old; 20–25 g) were purchased from Beijing Vital River Laboratory Animal Technology (Beijing, China). AgomiR-26a (80 mg/kg/day) and AAV9-sh-MIRF ( $1 \times 10^{11}$  vg/mouse) were injected into mice through the tail veins. Immediately after injection, the mice underwent MI or sham surgery. In brief, the mice were anesthetized using 1%–3% inhalant isoflurane and placed on a heating pad. Animals were intubated and ventilated with medical oxygen using a PhysioSuite MouseVent ventilator. The left anterior descending (LAD) coronary artery was visualized under a stereoscope and ligated using a 7-0 Prolene suture. Regional ischemia was confirmed by visual inspection under a stereoscope by discoloration of the occluded distal myocardium. Sham-operated animals were subjected to the same procedure without occlusion of the LAD. According to the time of MI duration in different groups, mice were anesthetized and hearts were collected. The procedures were in accordance with the regulations

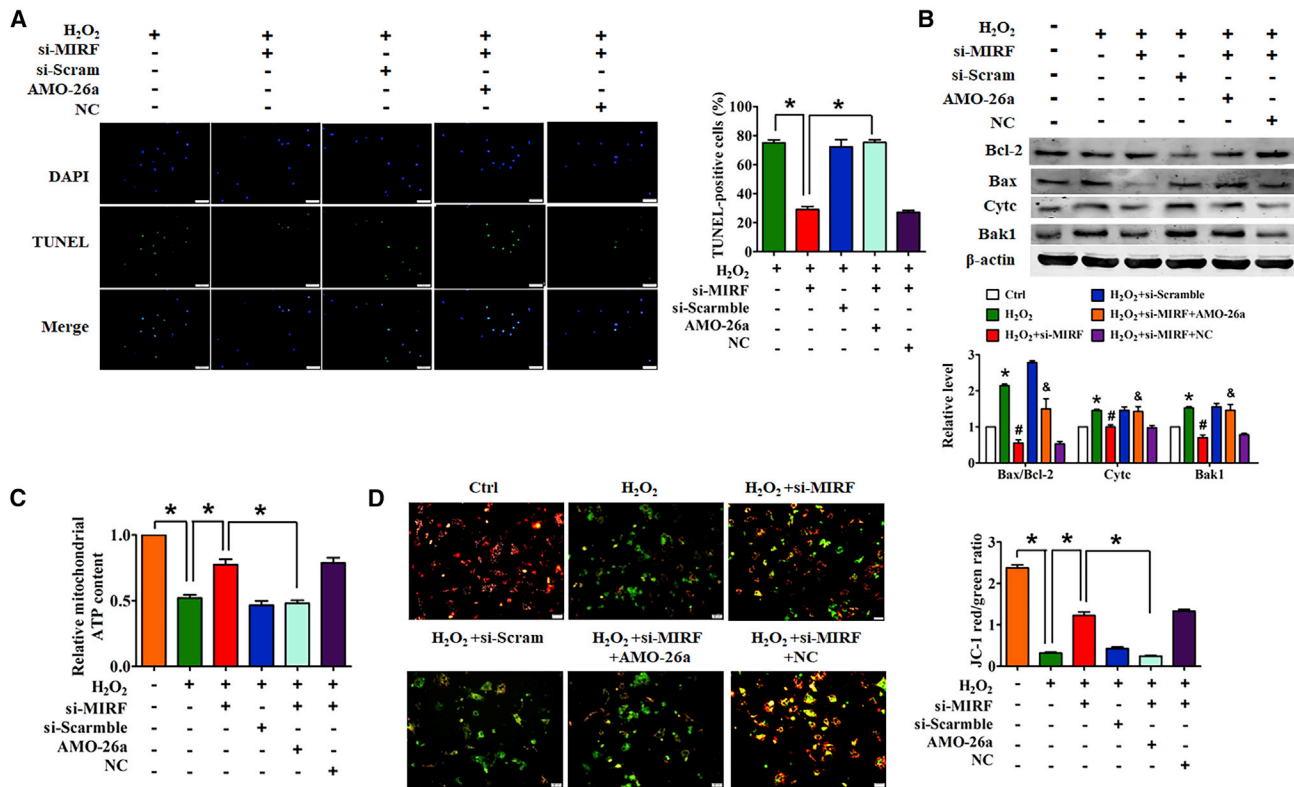


**Figure 6. Silencing MIRF Ameliorates H<sub>2</sub>O<sub>2</sub>-Induced Cardiomyocyte Injury through Modulating miR-26a**

(A) TUNEL staining indicated apoptotic cardiomyocytes. Treatment of H<sub>2</sub>O<sub>2</sub> increased TUNEL-positive cell numbers, which was reversed by si-MIRF, and AMO-26a abolished the effect of si-MIRF. \*p < 0.05. (B) Western blot analyzed the expression of Bcl-2, Bax, and Cytc in H<sub>2</sub>O<sub>2</sub>-treated NMCMs. n = 3; \*p < 0.05 versus Ctrl, #p < 0.05 versus H<sub>2</sub>O<sub>2</sub>, &p < 0.05 versus H<sub>2</sub>O<sub>2</sub>+si-MIRF. (C) Measurement of ATP content in cardiomyocytes, and ATP content was standardized by corresponding protein concentration. n = 4; \*p < 0.05. (D) JC-1 fluorescent probe was used to detect MMP, which indicated the function of mitochondria. \*p < 0.05.

of the Ethics Committee of Harbin Medical University and conformed to the *Guide for the Care and Use of Laboratory Animals* published by the US National Institutes of Health (NIH publication no. 85-23, 2011).

### TEM

Hearts slices were isolated and immediately fixed in 2.5% glutaraldehyde buffered with 0.1 M sodium cacodylate. Samples were post-fixed in 1% osmium tetroxide, dehydrated in ethanol, transitioned into propylene oxide, and then transferred into Epon/Araldite resin. Tissues were embedded into molds containing epoxy resin (Ladd Research Industries, Williston, VT, USA) and polymerized for 2 days at 65°C. 50-nm sections were placed onto carbon-coated Formvar slot grids and stained with aqueous uranyl acetate and lead citrate. A total of 60 tissue sections (eight fields of view per section) were observed via a transmission electron microscope (H-7650; Hitachi, Tokyo, Japan) at an accelerating voltage of 80 kV.

### Cell Culture and Transfection

Primary neonatal mice ventricular cardiomyocytes were isolated by dissociation of 1- to 3-day-old C57BL/6 mice. Cardiomyocytes were

cultured in Dulbecco's modified Eagle's medium (DMEM; HyClone, Logan, UT, USA) containing 10% fetal bovine serum (FBS; HyClone). Cardiomyocytes were transfected with miR-26a or AMO-26a and 2 μg MIRF or si-MIRF plasmid with Lipofectamine 2000 (Invitrogen, Carlsbad, CA, USA). Cardiomyocytes were exposed to 200 μM H<sub>2</sub>O<sub>2</sub> for 12 h to induce cardiomyocyte apoptosis.

### Quantitative Real-Time PCR

Total RNA was isolated from heart tissues or cultured cardiomyocytes using a TRIzol standard protocol (Invitrogen, Carlsbad, CA, USA). The concentration of RNA was examined by NanoDrop 8000 Spectrophotometer (Thermo Scientific, Wilmington, DE, USA). Reverse transcription of RNA into cDNA used High Capacity cDNA Reverse Transcription Kit (Applied Biosystems, Foster City, CA, USA). The relative expression levels of mRNAs and miRNAs were quantified by quantitative real-time PCR with SYBR Green I (Roche, Indianapolis, IN, USA). After circle reaction, the threshold cycle (Ct) was determined, and relative mRNA and miRNA levels were calculated based on the Ct values and normalized to β-actin or U6 level in each sample. The specific primers used in this study were shown as follows: U6 RT primer, 5'-CGCTTCACGAATTTGCGTGTTCAT-3';

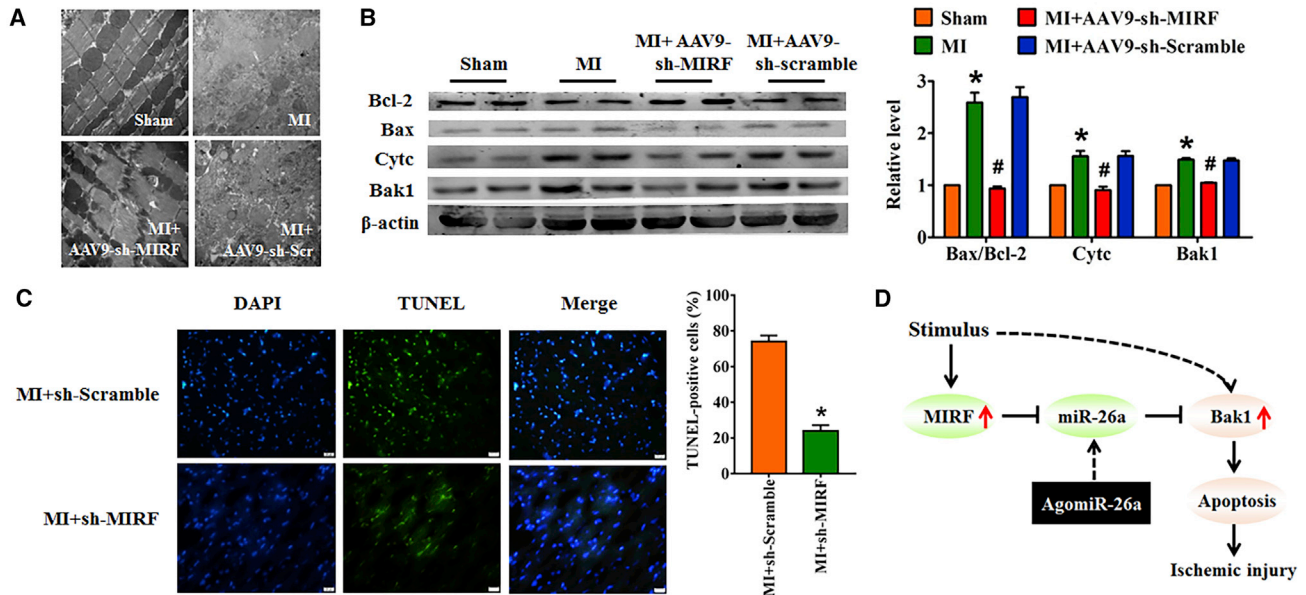


**Figure 7. Inhibition of MIRF Abrogated MI-Induced Apoptosis in Mice**

Mice were injected with AAV9-sh-MIRF and AAV9-sh-Scramble from the tail vein, then suffered from MI surgery at the seventh day after injection. (A) Representative TEM analyzed the ultrastructure of cardiomyocytes in the risk area of infarcted heart, including mitochondria, myofilament, and nucleus. (B) The protein levels of Bcl-2, Bax, Cytc, and Bak1 were measured by western blot.  $n = 4$ ; \* $p < 0.05$  versus sham, # $p < 0.05$  versus MI. (C) TUNEL staining indicated apoptotic cardiomyocytes. MI surgery increased TUNEL-positive cell numbers, which was reversed by AAV9-sh-MIRF injection. \* $p < 0.05$ ,  $n = 3$ . (D) Schematic model of MIRF modulating AMI through the miR-26a-Bak1 axis.

miR-26a RT primer, 5'-GTCGTATCCAGTGCCTGTCGTGGAGT CCGCAATTGCACTGGATACGACAGCCTAT-3'; U6 forward, 5'-CGCTTACGAATTTGCGTGCAT-3' and reverse, 5'-GCTTCGG CACATATACTAAAAT-3'; miR-26a forward, 5'-GCGTAGCAGC GGGAACAGT-3' and reverse, 5'-CCAGTGCCTGTCGTGGAG T-3'; MIRF forward, 5'-TCTTTCCAGTTCTCCTTGG-3' and reverse, 5'-GCAGTAGCAAATCCCCAAA-3'; Bak1 forward, 5'-CA GGATGGGGTCTCTACGAA-3' and reverse, 5'-GGGCTTTGGCT ACCGTCT-3'.

#### Protein Isolation and Western Blot

For western blot analysis, total protein samples were extracted from heart tissue or cardiomyocytes using radio-immunoprecipitation assay (RIPA) lysis buffer (Beyotime, Shanghai, China) with complete protease inhibitor cocktail (Roche Molecular Biochemicals, Basel, Switzerland). A total of 40–60  $\mu$ g proteins were fractionated on a 12% SDS-PAGE. After electrophoretically transferring to a Pure Nitrocellulose Blotting membrane (Pall Life Science), the blots were probed with primary antibodies, with  $\beta$ -actin (Proteintech, Wuhan, China) as a loading control. Primary antibodies included Bak1 (14673-1-AP; Proteintech), Bax (5099-2-Ig; Proteintech), Bcl-2 (12789-1-AP; Proteintech), and cytochrome *c* (10993-1-AP; Proteintech). The immunoreactivity was detected and analyzed using Odyssey Clx (Gene Company Limited, Hong Kong, China).

#### TUNEL Assay

TUNEL assay was used to evaluate cell apoptosis. Cells were plated on coverslips in 24-well culture plates. After 48 h of transfection, the cells

were performed using an *in situ* cell death detection kit (Roche, Mannheim, Germany) according to the manufacturer's protocol. The TUNEL-stained slides were washed with PBS and counterstained with 4',6-diamidino-2-phenylindole (DAPI; Beyotime, Shanghai, China). A fluorescence microscope (Olympus, Tokyo, Japan) was used to acquire the images. Nuclei that were double labeled with TUNEL and DAPI were considered to be TUNEL positive. The TUNEL-positive cells were counted in four non-overlapping microscopic fields of three independent experiments.

#### Luciferase Assay

HEK293 cells (American Type Culture Collection [ATCC], Manassas, VA, USA) were cultured in DMEM containing 10% FBS and 1% penicillin/streptomycin. HEK293 cells were co-transfected with WT Bak1 or mutant constructs and miR-26a, negative control, or AMO-26a. After 48 h of transfection, the cells were harvested and lysed. Luciferase activity was assayed using the Dual Luciferase Reporter Assay System (Promega, Mannheim, Germany) according to the manufacturer's instructions. Firefly luciferase values were normalized to Renilla, and relative ratios of Firefly to Renilla activity were reported.

#### JC-1 Assay

JC-1 assay was used to measure mitochondrial membrane permeability ( $\Delta\Psi_m$ ). The cardiomyocytes were assessed using the JC-1 assay kit (Beyotime, Shanghai, China), according to the manufacturer's instructions. Following treatment, the cells were incubated with the JC-1 stain in the dark at 37°C for 20 min and washed with

JC-1 buffer twice. The cells were subsequently observed under a fluorescence microscope (Olympus, Tokyo, Japan).

### Caspase-3 Activity Detection

Caspase-3/ CPP32 Colorimetric Assay Kit (Bio Vision, USA) was used to detect the activity of caspase-3. Then centrifuge lysis cells or tissues with lysis buffer to obtain supernatant. Dilute equivalent supernatant protein with lysis buffer to the reaction tube. Then add reaction buffer and DEVD-pNA substrate into the reaction tube at 37°C for 1 h. Detect the optical density at 405 nm in a microtiter plate reader.

### Statistical Analysis

All statistical analyses were performed using Prism software (GraphPad 5.0), and data are represented as mean ± SEM. Two groups were compared using Student's t tests. Multiple groups were compared using one- or two-way ANOVA test and Tukey's post hoc tests and repeated measures as indicated in the figure legends. Significance is defined as  $p < 0.05$ .

### AUTHOR CONTRIBUTIONS

H.L. conceived the ideas and designed the work. X.S. performed the experiments and drafted the manuscript. L.L., Y.L., R.F., R.Y., C.L., T.L., and D.Z. performed the experiments and analyzed the data. X.L., Y.Z., and H.S. provided suggestions about the experiments. L.L. and Y.L. revised the manuscript critically. All authors have read and approved the final manuscript.

### CONFLICTS OF INTEREST

The authors declare no competing interests.

### ACKNOWLEDGMENTS

This study was supported by the National Natural Science Foundation of China (grants 81770284 and 81673425); the Major Program of National Natural Science Foundation of China (grant 81730012); the Major Scientific Fund Project of Heilongjiang Province (grant ZD2019H001); the CAMS Innovation Fund for Medical Sciences (CIFMS; grant 2019-I2M-5-078); and the 2018 Heilongjiang Provincial University Fund of Basic Scientific Research (for L.L.).

### REFERENCES

- Hausenloy, D.J., Erik Botker, H., Condorelli, G., Ferdinandy, P., Garcia-Dorado, D., Heusch, G., Lecour, S., van Laake, L.W., Madonna, R., Ruiz-Meana, M., et al. (2013). Translating cardioprotection for patient benefit: position paper from the Working Group of Cellular Biology of the Heart of the European Society of Cardiology. *Cardiovasc. Res.* 98, 7–27.
- Ong, S.B., Hernández-Reséndiz, S., Crespo-Avilan, G.E., Mukhametshina, R.T., Kwek, X.Y., Cabrera-Fuentes, H.A., and Hausenloy, D.J. (2018). Inflammation following acute myocardial infarction: Multiple players, dynamic roles, and novel therapeutic opportunities. *Pharmacol. Ther.* 186, 73–87.
- Zhang, S., Lin, X., Li, G., Shen, X., Niu, D., Lu, G., Fu, X., Chen, Y., Cui, M., and Bai, Y. (2017). Knockout of Eva1a leads to rapid development of heart failure by impairing autophagy. *Cell Death Dis.* 8, e2586.
- Mátyás, C., Németh, B.T., Oláh, A., Török, M., Ruppert, M., Kellermayer, D., Barta, B.A., Szabó, G., Kókény, G., Horváth, E.M., et al. (2017). Prevention of the development of heart failure with preserved ejection fraction by the phosphodiesterase-5A inhibitor vardenafil in rats with type 2 diabetes. *Eur. J. Heart Fail.* 19, 326–336.
- Frangogiannis, N.G. (2015). Pathophysiology of Myocardial Infarction. *Compr. Physiol.* 5, 1841–1875.
- Zhou, Q., Li, L., Zhao, B., and Guan, K.L. (2015). The hippo pathway in heart development, regeneration, and diseases. *Circ. Res.* 116, 1431–1447.
- Nakamura, M., and Sadoshima, J. (2018). Mechanisms of physiological and pathological cardiac hypertrophy. *Nat. Rev. Cardiol.* 15, 387–407.
- Esteller, M. (2011). Non-coding RNAs in human disease. *Nat. Rev. Genet.* 12, 861–874.
- Li, L.J., Leng, R.X., Fan, Y.G., Pan, H.F., and Ye, D.Q. (2017). Translation of noncoding RNAs: Focus on lncRNAs, pri-miRNAs, and circRNAs. *Exp. Cell Res.* 361, 1–8.
- Zhang, J., Wang, P., Wan, L., Xu, S., and Pang, D. (2017). The emergence of noncoding RNAs as Heracles in autophagy. *Autophagy* 13, 1004–1024.
- Wang, K., Long, B., Zhou, L.Y., Liu, F., Zhou, Q.Y., Liu, C.Y., Fan, Y.Y., and Li, P.F. (2014). CARL lncRNA inhibits anoxia-induced mitochondrial fission and apoptosis in cardiomyocytes by impairing miR-539-dependent PHB2 downregulation. *Nat. Commun.* 5, 3596.
- Li, H.Q., Wu, Y.B., Yin, C.S., Chen, L., Zhang, Q., and Hu, L.Q. (2016). Obestatin attenuated doxorubicin-induced cardiomyopathy via enhancing long noncoding Mhrt RNA expression. *Biomed. Pharmacother.* 81, 474–481.
- Liu, Y., Zhou, D., Li, G., Ming, X., Tu, Y., Tian, J., Lu, H., and Yu, B. (2015). Long non coding RNA-UCA1 contributes to cardiomyocyte apoptosis by suppression of p27 expression. *Cell. Physiol. Biochem.* 35, 1986–1998.
- Brouwer, J.M., Lan, P., Cowan, A.D., Bernardini, J.P., Birkinshaw, R.W., van Delft, M.F., Sleebs, B.E., Robin, A.Y., Wardak, A., Tan, I.K., et al. (2017). Conversion of Bim-BH3 from Activator to Inhibitor of Bak through Structure-Based Design. *Mol. Cell* 68, 659–672.e9.
- Jiang, X., Li, L., Ying, Z., Pan, C., Huang, S., Li, L., Dai, M., Yan, B., Li, M., Jiang, H., et al. (2016). A Small Molecule That Protects the Integrity of the Electron Transfer Chain Blocks the Mitochondrial Apoptotic Pathway. *Mol. Cell* 63, 229–239.
- Karch, J., and Molkenin, J.D. (2015). Regulated necrotic cell death: the passive aggressive side of Bax and Bak. *Circ. Res.* 116, 1800–1809.
- Bayoumi, A.S., Park, K.M., Wang, Y., Teoh, J.P., Aonuma, T., Tang, Y., Su, H., Weintraub, N.L., and Kim, I.M. (2018). A carvedilol-responsive microRNA, miR-125b-5p protects the heart from acute myocardial infarction by repressing proapoptotic bak1 and klf13 in cardiomyocytes. *J. Mol. Cell. Cardiol.* 114, 72–82.
- Liang, H., Su, X., Wu, Q., Shan, H., Lv, L., Yu, T., Zhao, X., Sun, J., Yang, R., Zhang, L., et al. (2020). LncRNA 2810403D21Rik/Mirf promotes ischemic myocardial injury by regulating autophagy through targeting Mir26a. *Autophagy* 16, 1077–1091.
- Soleymanian, T., Kokabeh, Z., Ramaghi, R., Mahjoub, A., and Argani, H. (2017). Clinical outcomes and quality of life in hemodialysis diabetic patients versus non-diabetics. *J. Nephroptol.* 6, 81–89.
- Zidan, A., Awaisu, A., Kheir, N., Mahfoud, Z., Kaddoura, R., AlYafei, S., and El Hajj, M.S. (2016). Impact of a pharmacist-delivered discharge and follow-up intervention for patients with acute coronary syndromes in Qatar: a study protocol for a randomised controlled trial. *BMJ Open* 6, e012141.
- Dhingra, R., Gang, H., Wang, Y., Biala, A.K., Aviv, Y., Margulets, V., Tee, A., and Kirshenbaum, L.A. (2013). Bidirectional regulation of nuclear factor-κB and mammalian target of rapamycin signaling functionally links Bnip3 gene repression and cell survival of ventricular myocytes. *Circ. Heart Fail.* 6, 335–343.
- Yao, Y., Lu, Q., Hu, Z., Yu, Y., Chen, Q., and Wang, Q.K. (2017). A non-canonical pathway regulates ER stress signaling and blocks ER stress-induced apoptosis and heart failure. *Nat. Commun.* 8, 133.
- Wang, J.X., Gao, J., Ding, S.L., Wang, K., Jiao, J.Q., Wang, Y., Sun, T., Zhou, L.Y., Long, B., Zhang, X.J., et al. (2015). Oxidative Modification of miR-184 Enables It to Target Bcl-xL and Bcl-w. *Mol. Cell* 59, 50–61.
- Frankenreiter, S., Bednarczyk, P., Knies, A., Bork, N.L., Straubinger, J., Koprowski, P., Wrzosek, A., Mohr, E., Logan, A., Murphy, M.P., et al. (2017). cGMP-Elevating Compounds and Ischemic Conditioning Provide Cardioprotection Against Ischemia and Reperfusion Injury via Cardiomyocyte-Specific BK Channels. *Circulation* 136, 2337–2355.
- Tanimoto, T., Parseghian, M.H., Nakahara, T., Kawai, H., Narula, N., Kim, D., Nishimura, R., Weisbart, R.H., Chan, G., Richieri, R.A., et al. (2017).

- Cardioprotective Effects of HSP72 Administration on Ischemia-Reperfusion Injury. *J. Am. Coll. Cardiol.* *70*, 1479–1492.
26. Murakami, K. (2015). Non-coding RNAs and hypertension-unveiling unexpected mechanisms of hypertension by the dark matter of the genome. *Curr. Hypertens. Rev.* *11*, 80–90.
  27. Condorelli, G., Latronico, M.V., and Cavarretta, E. (2014). microRNAs in cardiovascular diseases: current knowledge and the road ahead. *J. Am. Coll. Cardiol.* *63*, 2177–2187.
  28. Cheng, Y., Zhu, P., Yang, J., Liu, X., Dong, S., Wang, X., Chun, B., Zhuang, J., and Zhang, C. (2010). Ischaemic preconditioning-regulated miR-21 protects heart against ischaemia/reperfusion injury via anti-apoptosis through its target PDCD4. *Cardiovasc. Res.* *87*, 431–439.
  29. Gazzaniga, F.S., and Blackburn, E.H. (2014). An antiapoptotic role for telomerase RNA in human immune cells independent of telomere integrity or telomerase enzymatic activity. *Blood* *124*, 3675–3684.
  30. Wu, T., Wu, D., Wu, Q., Zou, B., Huang, X., Cheng, X., Wu, Y., Hong, K., Li, P., Yang, R., et al. (2017). Knockdown of Long Non-Coding RNA-ZFAS1 Protects Cardiomyocytes Against Acute Myocardial Infarction Via Anti-Apoptosis by Regulating miR-150/CRP. *J. Cell. Biochem.* *118*, 3281–3289.
  31. Gong, L.C., Xu, H.M., Guo, G.L., Zhang, T., Shi, J.W., and Chang, C. (2017). Long Non-Coding RNA H19 Protects H9c2 Cells against Hypoxia-Induced Injury by Targeting MicroRNA-139. *Cell. Physiol. Biochem.* *44*, 857–869.